

Oxidation Kinetics by Water Vapor of Nuclear Graphite Grade 2114



Cristian Contescu
Yoonjo (Jo Jo) Lee
Robert Mee

November 2018

Approved for public release.
Distribution is unlimited.

DOCUMENT AVAILABILITY

Reports produced after January 1, 1996, are generally available free via US Department of Energy (DOE) SciTech Connect.

Website www.osti.gov

Reports produced before January 1, 1996, may be purchased by members of the public from the following source:

National Technical Information Service
5285 Port Royal Road
Springfield, VA 22161
Telephone 703-605-6000 (1-800-553-6847)
TDD 703-487-4639
Fax 703-605-6900
E-mail info@ntis.gov
Website <http://classic.ntis.gov/>

Reports are available to DOE employees, DOE contractors, Energy Technology Data Exchange representatives, and International Nuclear Information System representatives from the following source:

Office of Scientific and Technical Information
PO Box 62
Oak Ridge, TN 37831
Telephone 865-576-8401
Fax 865-576-5728
E-mail reports@osti.gov
Website <http://www.osti.gov/contact.html>

This report was prepared as an account of work sponsored by an agency of the United States Government. Neither the United States Government nor any agency thereof, nor any of their employees, makes any warranty, express or implied, or assumes any legal liability or responsibility for the accuracy, completeness, or usefulness of any information, apparatus, product, or process disclosed, or represents that its use would not infringe privately owned rights. Reference herein to any specific commercial product, process, or service by trade name, trademark, manufacturer, or otherwise, does not necessarily constitute or imply its endorsement, recommendation, or favoring by the United States Government or any agency thereof. The views and opinions of authors expressed herein do not necessarily state or reflect those of the United States Government or any agency thereof.

Materials Science and Technology Division

**OXIDATION KINETICS BY WATER VAPORS
OF NUCLEAR GRAPHITE GRADE 2114**

Cristian Contescu,¹ Yoonjo (Jo Jo) Lee,¹ and Robert Mee²

¹ Oak Ridge National Laboratory

² University of Tennessee, Knoxville

November 2018

Prepared by
OAK RIDGE NATIONAL LABORATORY
Oak Ridge, TN 37831-6283
managed by
UT-BATTELLE, LLC
for the
US DEPARTMENT OF ENERGY
under contract DE-AC05-00OR22725

This page was intentionally left blank

CONTENTS

	Page
LIST OF FIGURES	v
LIST OF TABLES.....	vii
ACRONYMS.....	ix
ABSTRACT.....	1
1. INTRODUCTION.....	3
2. MATERIALS AND PROCEDURES.....	5
2.1. GRAPHITE GRADE 2114	5
2.2. OXIDATION RATE MEASUREMENTS	6
2.3. DATA ANALYSIS.....	8
3. RESULTS.....	10
4. CONCLUSION.....	13
REFERENCES	14
APPENDIX A: PHYSICAL MEASUREMENTS AND TEST CONDITIONS.....	17
APPENDIX B: LOG OF EXPERIMENTAL RESULTS.....	19

This page was intentionally left blank

LIST OF FIGURES

Figure	Page
1. Optical microscopy image of graphite 2114 (polarized light)	5
2. Schematic showing the cutting diagram for oxidation specimens.....	6
3. Schematic of the experimental setup used for graphite oxidation measurements.....	7
4. Four views of the thermogravimetric apparatus and auxiliary gas lines and instruments.....	8
5. Experimental oxidation rates at $P_{H_2} = 0$ and trends predicted by two kinetic models	11
6. Temperature variation of apparent reaction order $m(T)$	11
7. Measured and predicted oxidation rates using the classical LH and the new BLH model	12

This page was intentionally left blank

ACRONYMS

ASTM	American Society for Testing and Materials
BLH	Boltzmann-Langmuir-Hinshelwood (kinetic model)
GA	General Atomics (company)
HTGR	High Temperature Gas-cooled Reactor
LH	Langmuir-Hinshelwood (kinetic model)
ORNL	Oak Ridge National Laboratory
SSE	sum of squared errors
TAG	Thermo-analyseur gravimmetrique / gravimetric thermoanalyzer (instrument)
TPD	temperature-programmed desorption
TPO	temperature-programmed oxidation
VHTR	Very High Temperature Reactor

This page was intentionally left blank

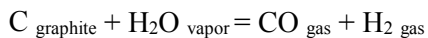
ABSTRACT

This report presents measurement results of oxidation rates by water vapor of nuclear graphite grade 2114 manufactured by Mersen, USA. This report completes kinetic study of chronic oxidation of grade 2114, of which partial data were compiled as a Letter Report in July 2017. The research is part of a broader program at Oak Ridge National Laboratory (ORNL) aiming at development of a comprehensive model for chronic oxidation of nuclear graphite in conditions relevant to operation of gas-cooled high-temperature reactors (HTGR). Grade 2114 is the fourth nuclear graphite investigated under this program. Experimental data measured at ORNL were analyzed in collaboration with Dr. Robert Mee (University of Tennessee, Knoxville) and graphite-specific parameters in the oxidation rate equation were determined. It was shown, once again, that the new Boltzmann-enhanced Langmuir-Hinshelwood (BLH) model recently proposed by ORNL is a better choice than the classical Langmuir-Hinshelwood (LH) model for prediction of chronic oxidation of graphite components during normal operation of HTGRs.

This page was intentionally left blank

1. INTRODUCTION

Graphite is used as a moderator and structural material in high temperature gas-cooled reactors (HTGR). Although stable in reducing environments, graphite is susceptible to oxidation by traces of oxygen, water, and carbon dioxide that might be present in the helium coolant at the operating temperatures (about 700 – 950 °C). Even though the coolant chemical composition is strictly controlled, water (moisture) is the most difficult gas species to remove. Depending on specific HTGR design, the water vapor partial pressure may vary from about 5 Pa (Fort St. Vrain, USA, 1976-1979) to 0.2 Pa (Dragon, UK, 1964-1975), with most common values grouped around 1.1 – 1.4 Pa (Peach Bottom, USA, 1967-1974; HTTR, Japan, 1999; HTR-10 China, 2003; and HTR-PM project, China) at total helium pressures of 4 – 9 MPa [1-6]. Over several decades of lifetime, it is inevitable that extremely slow, but continuous (chronic) oxidation of graphite will occur at high temperatures. The reaction products for oxidation by water are hydrogen and carbon monoxide. Their presence in the gas phase in contact with the graphite (or in graphite's pores) can shift the equilibrium and slow down the reaction rate:



This chronic graphite gasification may slowly but surely corrode the fuel elements and other structural components in the core, weakening their mechanical strength and potentially jeopardizing the reactor integrity. Early analysis of chronic oxidation effects was performed at General Atomics (GA) in the 1970's based on accelerated oxidation tests of graphite grade H-451, which at the time was the U. S. graphite candidate for gas-cooled reactors [7]. H-451 is medium fine-grain size (1.25 mm) extruded graphite manufactured from a petroleum precursor by Great Lakes Carbon in United States.¹ The GA report [8] contains carefully measured oxidation rates in helium with controlled amounts of moisture and hydrogen. By fitting the observations to the kinetic model proposed by Langmuir, Hinshelwood and others (LH) [8] the authors provided numerical values of three kinetic constants and their temperature variation. Building on these results, Richards [9] analyzed water transport in porous graphite and its depletion by the oxidation reaction. He concluded that corrosion by moisture will affect only a thin layer (about 1-2 mm) at the surface of graphite components, provided the steam concentration in the HTGR coolant is kept below 0.1 ppm at a total design pressure of 63 atm (less than 6.4 Pa partial pressure) [9]. This prediction was cross-validated against unpublished density measurements made in Germany on graphite grade 2020 oxidized by water. The latter is fine grain (0.015 mm) graphite with completely different microstructure than the medium grain H-451.

The raw material used for fabrication of graphite H-451 is no longer available. With the resurgence of interest in large and modular HTGR systems, new graphite grades are now considered for potential use. They have different precursors, fabrication techniques, and various structures with either small or medium grain sizes. It is well known by now that graphite microstructure has a strong effect on oxidation behavior [10-13]. Yet, for lack of information on oxidation behavior of the new graphite grades, reactor design and

¹ This report uses the latest classification of nuclear graphite grades based on their grain size (ASTM D8075-16, "Standard guide for Categorization of microstructural and microtextural features observed in optical micrographs of graphite").

HTGR safety analysis continues to use the LH kinetic model with the parameters [7] specific to graphite H-451 [14-19]. Based on the current knowledge on graphite properties there are strong reasons to question whether extrapolating oxidation behavior of one graphite grade to another grade, with different origin and physical properties, and then using that as the design basis for reactor safety qualification, is the right thing to do. The stricter requirements of regulatory bodies demand that safety analysis is based on actual properties of each material loaded in the reactor. There is a strong need for proper characterization of chronic oxidation behavior of new grades of nuclear graphite proposed as candidates for HTGR and the very high temperature reactor (VHTR).

Investigation of nuclear graphite chronic oxidation by moisture was initiated at Oak Ridge National Laboratory in 2012. A large amount of experimental data was collected in the past few years on oxidation kinetics of medium fine-grained graphite (PCEA and NBG-17) and one superfine-graded graphite (IG-110). This work continued with the study of a second fine grain graphite (2114). Partial results from this study were presented in electronic letter report form to Idaho National Laboratory in July 2017 [20]. It was shown again that a new kinetic model [21,22] proposed first in 2016 is better suited than the classical LH model for representation of oxidation rates by moisture measured at very different conditions. The new Boltzmann-enhanced Langmuir-Hinshelwood (BLH) rate equation is a semi-global kinetic model [23] derived from the classical LH equation but enhanced with a temperature-dependent reaction order described by a Boltzmann distribution [22].

2. MATERIALS AND PROCEDURE

2.1 GRAPHITE GRADE 2114

Graphite 2114 is superfine grained isotropic graphite manufactured by isostatic molding by Mersen, USA (former Carbone Lorraine). It is considered a possible candidate for use in HTGRs. According to manufacturer's specification [24], this graphite has an average grain size of 13 μm , low porosity (10 %), cumulative pore volume of only 7 mm^3/g , and the majority of pores with sizes lower than 1 μm . Figure 1 shows an optical microscopy mosaic image of this material recorded with polarized light. The image size is 1 mm x 1 mm.

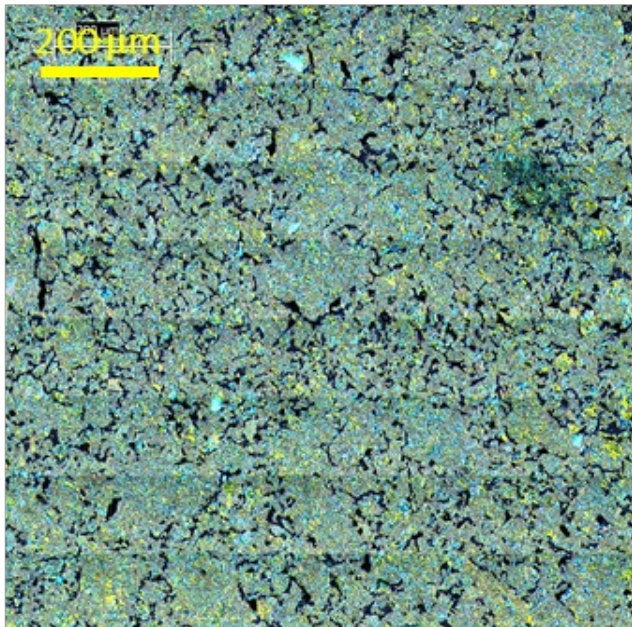


Figure 1: Optical microscopy image of graphite 2114 (polarized light)

Graphite specimens for oxidation studies were machined from two square bars cut from billet 101103 of grade 2114 acquired from Mersen. The cutting scheme is shown in Figure 2. A subsection of bar 2 (labeled sub-bar 2A) was used for machining of thin graphite slabs used for effective diffusivity measurements that will be reported in another document. The specimens used for oxidation studies were cylinders (25 mm length \times 5 mm diameter). A hole (0.75 mm diameter) near one end was used for suspension with a platinum wire in the thermogravimetric apparatus.

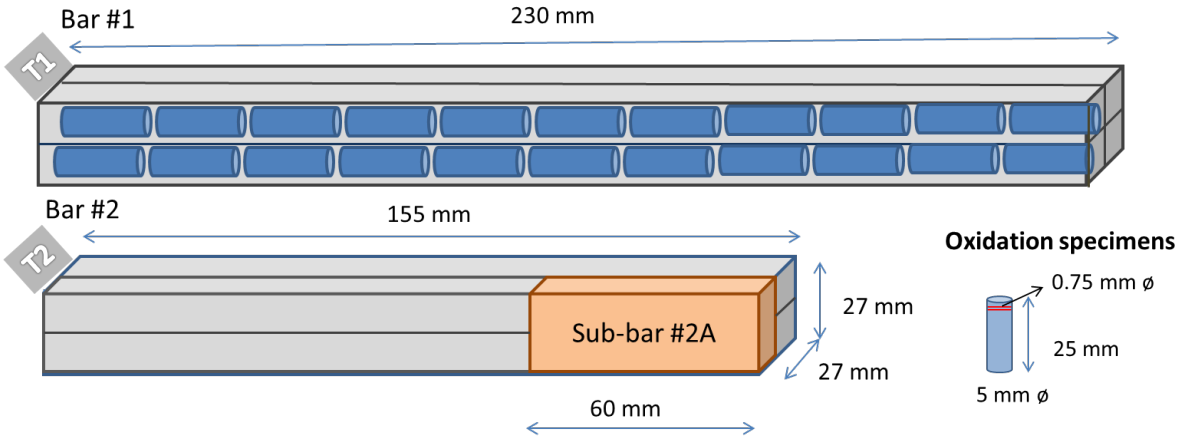


Figure 2: Schematic showing the cutting diagram for oxidation specimens. Sub-bar 2A was used for machining the graphite slabs used for water diffusivity measurements.

2.2. OXIDATION RATE MEASUREMENTS

Oxidation rates were measured in the dual symmetrical thermogravimetric analyzer TAG 16/18 (Setaram, France). This instrument has a resolution of $0.5 \mu\text{g}$ and excellent temperature control. Details on the experimental setup can be found elsewhere [21,25-27]. In summary, graphite cylinders (25 mm long, 5 mm diameter) were oxidized at constant flow conditions (1.5 L/min, atmospheric pressure) using ultrahigh purity helium (> 99.999 vol. %) containing controlled partial pressures of water vapor ($3 < P_{\text{H}_2\text{O}} < 1200 \text{ Pa}$) and hydrogen ($0 < P_{\text{H}_2} < 150 \text{ Pa}$). Oxidation rates were obtained from the weight loss during 3 hours of exposure at constant temperature (between 800 and 1100 °C) and were normalized to the actual weight of the specimens. Fresh specimens were used for every new set of gas composition ($P_{\text{H}_2\text{O}}$, P_{H_2}). With gas composition held fixed, the temperature was raised stepwise from the lowest to the highest in 50 °C increments. Each specimen was tested at as many of 7 temperatures. Gas compositions were adjusted by varying the flow rate ratios between a flow of dry He, a second flow of He humidified in a controlled temperature bubbler, and (occasionally) a third flow of dry 1% H₂ / balance He. Gas flow rates of each gas stream were measured by calibrated mass flow controllers which were adjusted and recorded by a LabView application. The same application controlled the water bath temperature and recorded barometric pressure in the laboratory. The moisture content of reunited gas flows was measured just before the inlet port of the thermogravimetric balance by a precision chilled mirror hygrometer. Figure 3 shows a schematic of the experimental setup. The final weight loss for each specimen was not higher than 1 %. It was assumed that oxidation was in the chemical control regime and the rates measured were essentially not affected by diffusion. All gases were ultrahigh purity grade and the water for steam generation was ultra-high purity plasma-grade. The hydrogen concentration in the H₂/He mixture was certified by the gas mixture provider (AirGas) and the concentration of H₂ in the oxidation chamber was calculated from the flow rate values.

Physical measurements data for the 47 graphite specimens used in this study, along with the test conditions employed, are provided in Appendix A.

Setup for graphite oxidation in H₂O-He mixtures

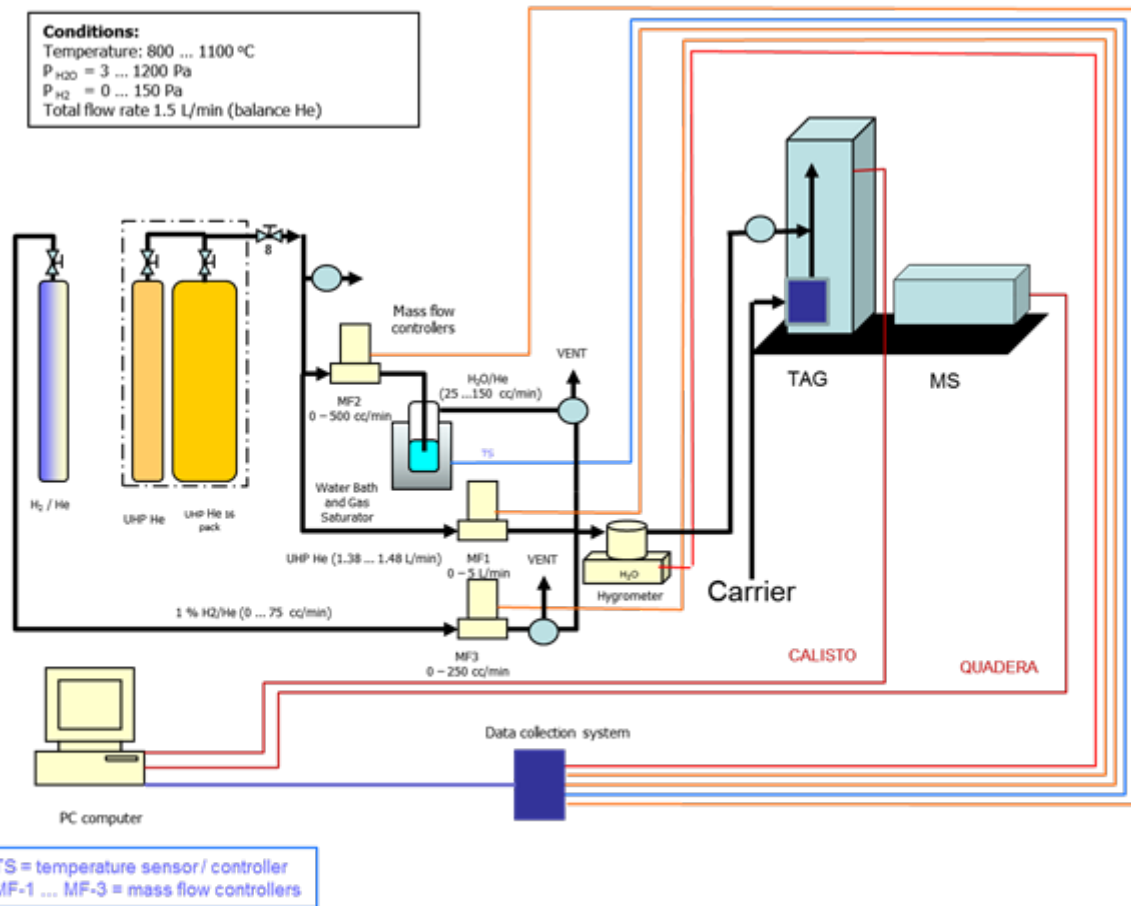


Figure 3: Schematic of the experimental setup used for graphite oxidation measurements.

Figure 4 shows a general view of the equipment, details of the gas lines with the hygrometer and the water bath used for helium humidification, and two views of the TAG instrument with the dual furnace in the lowered position. The graphite specimen is attached to one arm of the microbalance (right side) and the other arm (left side) holds a reference quartz cylinder with the same volume as the graphite specimen. This symmetrical construction allows for fine compensation of gas buoyancy that always occurs in a flow system. Although temperature variations caused apparent weight variations in the system (related to gas density variations), in isothermal conditions the quartz reference maintains stable weight, allowing for accurate measurements of weight changes of the graphite samples.

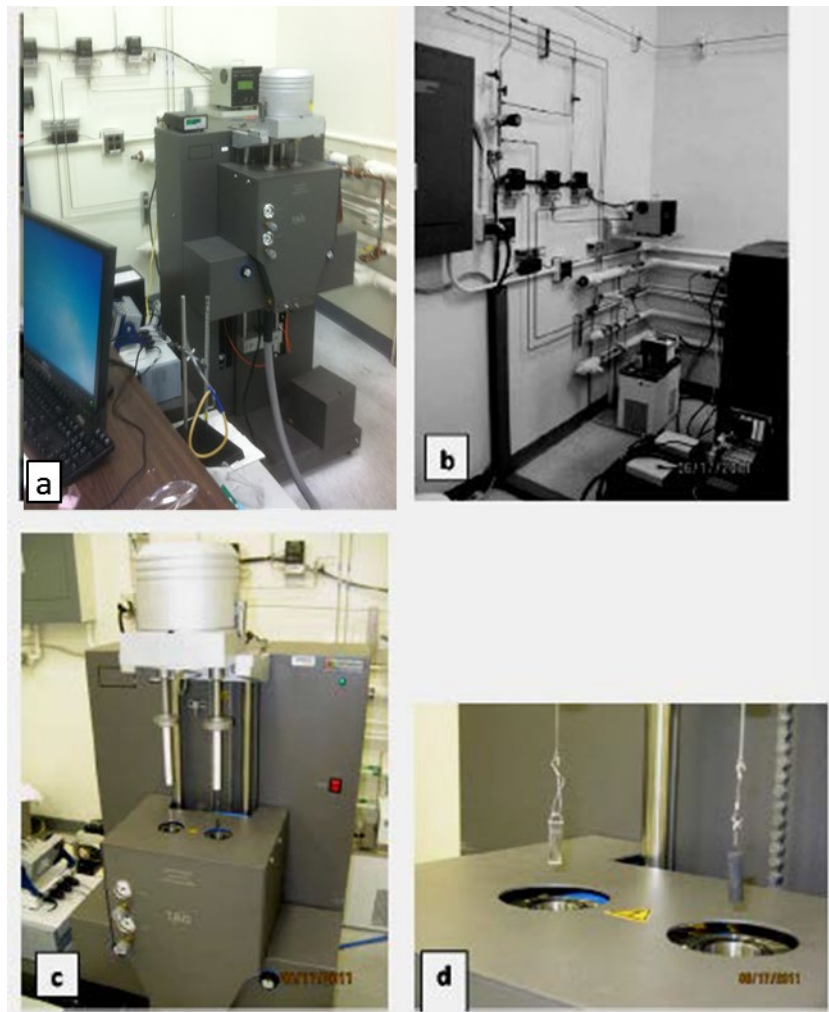


Figure 4: Four views of the thermogravimetric apparatus and auxiliary gas lines and instruments: (a) general view; (b) gas lines, water bath humidifier and hygrometer; (c) open furnace showing the two arms of the symmetrical balance; (d) graphite specimen (right) and quartz reference (left) attached to the high sensitivity microbalance through Pt wires and hanging rods

2.3. DATA ANALYSIS

Two hundred eighty-seven rate values were collected at various gas compositions and temperatures. A small number of observations were invalidated because of experimental errors, more frequently encountered for very low oxidation rates that were sometimes below the sensitivity limit of the equipment. All valid data were simultaneously analyzed by solving a set of multiple non-linear rate equations (to be introduced below) from which the most probable parameter values were found by minimization of the sum of squared errors (SSE) for $Y = \log(Rate)$ where Y is the rate measured at any given condition. Two different rate equations were used for data analysis, as follows:

- Classical Langmuir-Hinshelwood (LH) equation [7,8]:

$$\text{Rate}_{\text{LH}}(P_{\text{H}_2\text{O}}, P_{\text{H}_2}, T) = \frac{k_1 P_{\text{H}_2\text{O}}}{1 + k_2 (P_{\text{H}_2})^{0.5} + k_3 P_{\text{H}_2\text{O}}} \quad (1)$$

$$\text{where } k_i = A_i \exp\left(-\frac{E_i}{RT}\right) \quad (1a)$$

In these equations *Rate* is weight-normalized oxidation rate ($\text{mg}_{\text{oxidized}} / \text{mg}_{\text{initial}} / \text{s}$, or s^{-1}), T is the temperature (K), E is the activation energy (J mol^{-1}), and R is the gas constant ($8.314 \text{ J mol}^{-1} \text{ K}^{-1}$). This kinetic model has six parameters which must be estimated by fitting all data: three preexponential factors (A_i , $i = 1, 2, 3$) and three apparent activation energies (E_i , $i = 1, 2, 3$).

- The Boltzmann-enhanced Langmuir-Hinshelwood model [21,22]:

$$\text{Rate}_{\text{BLH}}(P_{\text{H}_2\text{O}}, P_{\text{H}_2}, T) = \frac{k_1 (P_{\text{H}_2\text{O}})^{m(T)}}{1 + k_2 (P_{\text{H}_2})^{0.5} + k_3 (P_{\text{H}_2\text{O}})^{m(T)}} \quad (2)$$

$$\text{where } k_i = A_i \exp\left(-\frac{E_i}{RT}\right) \quad \text{and} \quad m(T) = m_{\max} + \frac{m_{\min} - m_{\max}}{1 + \exp\left(\frac{T - T_o}{\theta}\right)} \quad (2a)$$

This new BLH kinetic model [21,22] accounts for faster increase of oxidation rates at high water vapor pressure ($>100 \text{ Pa}$) and high temperatures ($>950 \text{ }^{\circ}\text{C}$) than what is predicted by the LH model. Differences between the experimental rates and those predicted by the LH model were also observed in prior studies on medium grain (PCEA, NBG-17) and superfine grain (IG-110) graphite in the same range of oxidant pressures and temperatures [22]. To represent all data by a unique, more robust model, a correction was introduced in the BLH model, by assuming that the reaction order for oxidant (water) depends on temperature, $m(T)$. This dependence, expressed by eq. (2a), was best modeled by the integral Boltzmann distribution function, with four new parameters: m_{\min} and m_{\max} that define the range of apparent reaction order, T_o which is a characteristic temperature associated with the inflection of $m(T)$ function, and θ which is a scaling parameter equal to the inverse slope of $m(T)$ at T_o . With these changes, the BLH model has ten parameters that must be estimated from the collected data.

3. RESULTS

The table in Appendix B contains all oxidation rate data and their corresponding experimental conditions. Figure 5 shows some of the experimental reaction rates (only those measured at $P_{H_2} = 0$) as a function of P_{H_2O} and temperature. These data (and those measured in mixtures containing H_2O and H_2) were fitted with the analytical expressions shown below, which were obtained by combining eqs. (1) and (1a), and respectively (2) and (2a):

$$\text{Rate}_{\text{LH}} = \frac{a_1 \exp\left(-\frac{E_1}{RT}\right)(P_{H_2O})}{1 + A_2 \exp\left(-\frac{E_2}{RT}\right)(P_{H_2})^{0.5} + A_3 \exp\left(-\frac{E_3}{RT}\right)(P_{H_2O})} \quad (3)$$

$$\text{Rate}_{\text{BLH}} = \frac{\frac{A_1 \exp\left(-\frac{E_1}{RT}\right)(P_{H_2O})}{1 + A_2 \exp\left(-\frac{E_2}{RT}\right)(P_{H_2})^{0.5} + A_3 \exp\left(-\frac{E_3}{RT}\right)(P_{H_2O})} \left[m_{\max} - \frac{m_{\max} - m_{\min}}{1 + \exp\left(\frac{T - T_0}{\theta}\right)} \right]}{1 + A_2 \exp\left(-\frac{E_2}{RT}\right)(P_{H_2})^{0.5} + A_3 \exp\left(-\frac{E_3}{RT}\right)(P_{H_2O})} \quad (4)$$

All parameters determined from best fit of the two models are listed in Table 1. The least squares analysis was based on minimization of the sum of squared errors for $\ln(\text{Rate})$. The isothermal trends calculated with the best fitted parameters from these models are also plotted, at each temperature, in Figure 5. It is immediately seen that the LH model cannot reproduce fast oxidation rates at high water pressures ($P_{H_2O} > 100$ Pa) and high temperatures ($T > 950$ °C). Moreover, the trend predicted by the LH model is too conservative. According to this model, the oxidation rates would reach asymptotically a constant value when P_{H_2O} increases. That maximum rate would be dependent only on temperature (Fig. 5, top panel). In contrast, the experimental data show a different behavior, incompatible with the LH model for rates approaching the maximum rate. The oxidation rates continue to increase with P_{H_2O} and the rate of their variation (the slope on double logarithmic representations of Fig. 5) depends on temperature. This supports the hypothesis that the reaction order for water depends on temperature. The observed apparent reaction orders calculated from experimental data are plotted versus temperature in Figure 6. This sigmoidal dependence on temperature is accurately reproduced by the integral Boltzmann distribution function. The explicit expression of $m(T)$ is shown above, eq. (2a). In contrast, the LH model predicts for the same data just a slow linear variation with temperature, which evidently is not observed experimentally.

Table 1: Temperature variation of kinetic constants defined in Eqs. (1) and (2) for LH and BLH models, respectively

	LH model	BLH model
k_1	$3.89\text{E-}07 \times \exp(-57800/R\ T)$	$9.13\text{E-}12 \times \exp(61380/R\ T)$
k_2	$2.56\text{E-}02 \times \exp(23920/R\ T)$	$1.47\text{E+}00 \times \exp(-1650/R\ T)$
k_3	$4.91\text{E-}09 \times \exp(167230/R\ T)$	$3.38\text{E-}14 \times \exp(280600/R\ T)$
$m(T)$		$1.463 - 1.400/[1 + \exp((T - 1288)/39.8)]$

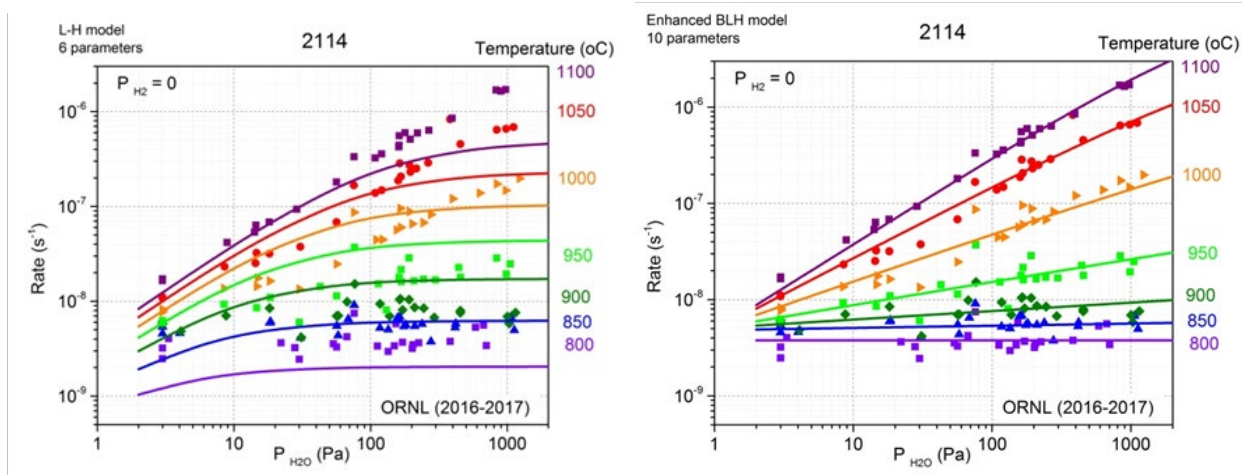


Figure 5: Experimental oxidation rates at $P_{\text{H}_2} = 0$ and trends predicted by two kinetic models: LH (left) and BLH (right)

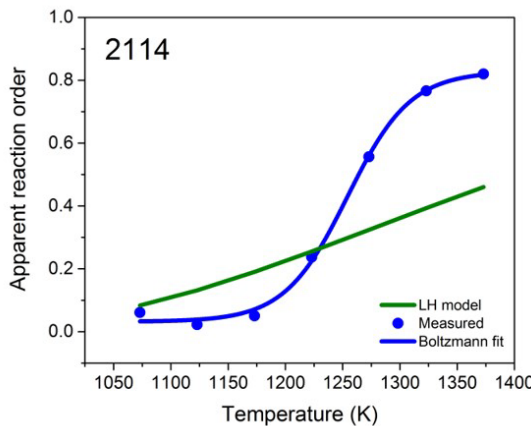


Figure 6: Temperature variation of apparent reaction order $m(T)$. Data based on observed oxidation rates are shown by symbols, along with their fit by the Boltzmann distribution function, eq. (2). The LH model predicts, for the same data, a linear dependence which is not observed experimentally.

Figure 7 compares the quality of fit afforded by the LH and BLH models. The double logarithmic plots show observed and predicted rate values in experiments with water only (blue symbols) and with water with hydrogen added (red symbols). The higher the correlation coefficient between observed and predicted rates, the better the fit. With the data available, the correlation coefficient calculated for the LH model is only $R^2 = 0.79$, but it is $R^2 = 0.91$ for the BLH model. The BLH model reproduces the measured rates better than the LH model and can therefore be used with greater confidence for prediction of oxidation rates. There is some data scattering in the range of low oxidation rates, especially in experiments with hydrogen added. The scattering is observed for both kinetic models, but it is larger for the LH model and smaller for the BLH model.

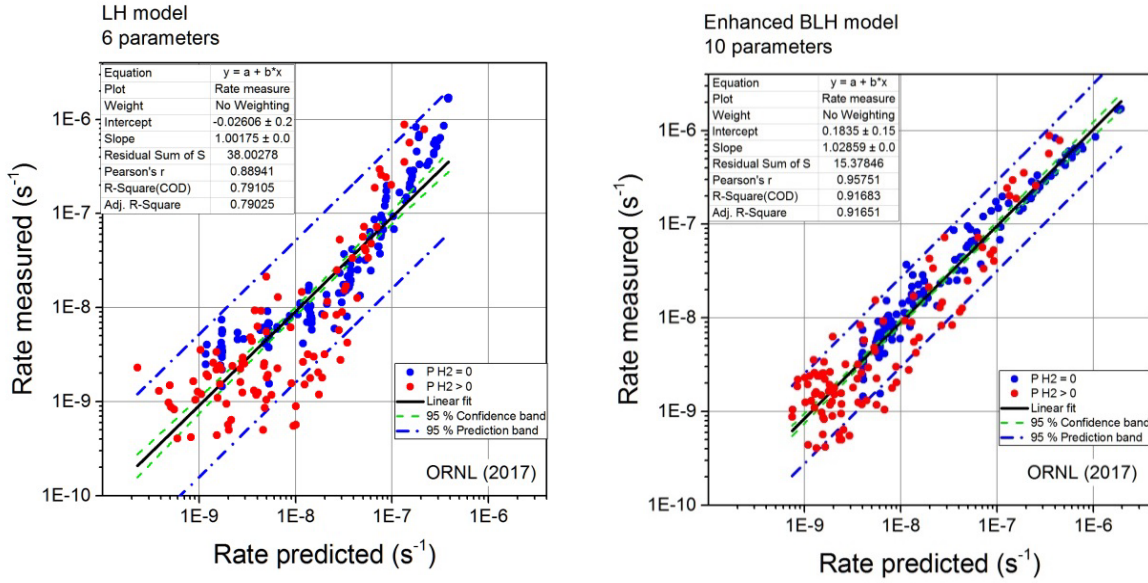


Figure 7: Measured and predicted oxidation rates using the classical LH model (left) and the new BLH model (right). Blue symbols are for oxidation by moisture only and red symbols for oxidation by moisture with added hydrogen.

4. CONCLUSION

The work presented in this report is part of a larger program, aimed at characterization of chronic effects caused by oxidation by moisture of the new grades of graphite that can be potentially used in HTGRs. The results from current kinetic experiments with graphite 2114 adds new information to a series of similar results obtained for grades PCEA, NBG-17, and IG-110 in previous years [21,22]. This work is inevitably slow because oxidation by water is an extremely slow process. Kinetics is explored through a large number of accelerated oxidation tests, where measured rates are tens or hundreds of times faster than the expected rates under HTGR operating conditions. The underlying assumption of the study is that accurate characterization of effects of high water and hydrogen concentrations can be used to deduce the behavior at pressures too low for direct measurements. Variability of local properties in graphite and the experimental errors (enhanced in slow oxidation conditions) require that data analysis is based on a statistically significant population of observables. In the course of the project it became clear that the classical LH model cannot reproduce consistently all observations, and that the rates measured at high temperatures and large water partial pressures are actually faster than predicted by the LH model. The new BLH model is a more robust mathematical tool for prediction of oxidation rates over broad ranges of temperatures and water and hydrogen partial pressures.

All oxidation rate measurements are now completed for four grades of graphite (medium grained PCEA and NBG-17, and superfine gained IG-110 and 2114). The project continues with characterization of density profiles in specimens oxidized nonuniformly at well-defined conditions, and measurements of effective diffusivity coefficients of water vapor in the four grades of graphite. When all this information is available, it will be possible to develop comparative predictions on the behavior of these graphites in the HTGRs and to verify these predictions through direct measurements.

REFERENCES

1. M P Kissane, A review of radionuclide behavior in the primary system of a very-high temperature reactor, *Nucl. Eng. Design*, **239** (2009) 3076–3091.
2. X Yu, S Yu, Analysis of fuel element matrix graphite corrosion in HTR-PM for normal operating conditions, *Nucl. Eng. Design*, **240** (2010) 738–743.
3. E R Corwin, Generation IV Reactors Integrated Materials Technology Program Plan: Focus on Very High Temperature Reactor Materials, ORNL/TM-2008/129 (2008).
4. H G Olson, H L Brey, The Fort Saint Vrain high temperature gas cooled reactor, VI Evaluation and removal of primary coolant contaminants, *Nucl Eng. Design* 61 (1980) 315-322.
5. B Castle, NGNP Reactor Coolant Chemistry Control Study, INL/EXT-10-10533.
6. R N Wright, Kinetics of Gas Reactions and Environmental Degradation in NGNP Helium, INL/EXT-06-11494.
7. C Velasquez, G Hightower, R Burnette, The Oxidation of H-451 Graphite by Steam. Part 1: Reaction Kinetics, General Atomic Company, GA-A14951 (1978).
8. P L Walker, Jr, F Rusinko, Jr, L G Austin, Gas Reactions of Carbon, *Adv. Catalysis* **11** (1959) 133-221.
9. M B Richards, Reaction of nuclear grade graphite with low concentrations of steam in the helium coolant of an MHTGR, *Energy* **15** (1990) 729-739.
10. C. I. Contescu, T. Guldan, P. Wang, T. D. Burchell, The effect of microstructure on air oxidation resistance of nuclear graphite, *Carbon* **50** (2012) 3354-3366.
11. W-K Choi, B-J Kim, E-S Kim, S-H Chi, S-J Park, Oxidation behavior of IG and NBG graphites, *Nucl Eng Design*, **241** (2011) 82-87.
12. M S El-Genk, J-M P Tournier, Comparison of oxidation model predictions with gasification data of IG-110, IG-430 and NBG-25 nuclear graphite, *J Nucl Mater* **429** (2012) 141-158.
13. W-H Huang, S-C Tsai, C-W Yang, J-J Kai, The relationship between microstructure and oxidation effects of selected IG- and NBG-grade nuclear graphites, *J Nucl Mater* **454** (2014) 149-158.
14. M Eto, T Kurosawa, Estimation of graphite materials corrosion with water-vapor in coolant of VHTR and oxidation effect on the materials properties. Specialists' Meeting on Graphite Component Structural Design. JAERI Tokai (Japan) September 8-11, 1986, IWGGR-11: 189-194.
15. X Yu, L Brissoneau, C Bourdeloie, S Yu, The modeling of graphite oxidation behavior for HTGR fuel coolant channels under normal operating conditions, *Nucl Eng Design* **238** (2008) 2230-2238.
16. X Luo, X Yu, S Yu, J-C Robin, Analysis of graphite gasification by water vapor at different conversions, *Nucl Eng Design* **273** (2014) 68-74.
17. M M Stempniewicz, Correlation for steam-graphite reaction, *Nucl Eng Design* **280** (2014) 287-293.
18. Yu, S Yu, Analysis of fuel element matrix graphite corrosion in HTR-PM for normal operating conditions, *Nucl Eng Design* **240** (2010) 738-743.
19. M Richards, REACT_COMPACT: A computer code for modeling graphite corrosion and fuel hydrolysis, in HTR2016, International Topical Meeting on High Temperature Reactor Technology, Las Vegas, NV, November 6-10, 2016.
20. C I Contescu, Current progress in determining oxidation results of graphite grade 2114, Electronic Letter Report submitted to Idaho National Laboratory in completion of deliverable 4.3.A according to HTR Graphite R&D ORNL FY 2017 MPO (July 2017).
21. C I Contescu, R Mee, Status of chronic oxidation studies of graphite, ORNL/TM-2016/195.

22. C I Contescu, R W Mee, Y (JJ) Lee, J D Arregui-Mena, N C Gallego, T D Burchell, J J Kane, W E Windes, Beyond the classical kinetic model for chronic graphite oxidation by moisture in high-temperature gas-cooled reactors, *Carbon* 127 (2018) 158-169; 140 (2018) 249.
23. T H Hurt, J M Calo, Semi-global intrinsic kinetics for char combustion modeling, *Combustion and Flame*, **125** (2001) 138-1149.
24. https://www.graphite-eng.com/uploads/downloads/continuous_casting_brochure.pdf (accessed 10/17/2018).
25. C. I. Contescu, T. D. Burchell, R. W. Mee, Accelerated oxidation studies of PCEA nuclear graphite by low concentrations of water and hydrogen in helium, ORNL/TM-2013/524 (2013).
26. C.I. Contescu, R.W. Mee, P. Wang, A.V. Romanova, T.D. Burchell, Oxidation of PCEA nuclear graphite by low water concentrations in helium, *J. Nucl. Mater.* **453** (2014) 225-232.
27. C.I. Contescu, T.D. Burchell, R.W. Mee, Kinetics of chronic oxidation of NBG-17 nuclear graphite by water vapor, ORNL/TM-2015/142 (2015).

This page was intentionally left blank

APPENDIX A
PHYSICAL MEASUREMENTS AND TEST CONDITIONS

Test Date	Specimen ID	BEFORE TEST			CONDITIONS			AFTER TEST		
		Weight mg	Average L mm	Average D mm	Density g/cm ³	P _{H₂O} Pa	P _{H₂} Pa	Weight mg	Average L mm	Average D mm
11/16/2016	M-1	897.15	25.01	5.01	1.825	200	0	886.86	25.00	5.01
11/21/2016	M-2	901.27	25.01	5.02	1.821	200	0	891.55	25.00	5.01
11/23/2016	M-3	901.67	25.00	5.02	1.827	100	0	895.75	25.01	5.02
11/30/2016	M-4	900.32	24.99	5.01	1.827	50	0	897.08	25.00	5.01
12/15/2016	M-5	886.41	24.99	4.99	1.813	150	0	879.12	24.99	4.99
12/19/2016	M-6	895.45	25.02	5.01	1.819	25	0	893.77	25.02	5.01
12/21/2016	M-7	886.86	25.01	5.00	1.805	500	0	881.11	25.00	5.00
1/9/2017	M-8	900.43	25.01	5.00	1.832	25	0	898.69	25.02	5.01
1/11/2017	M-9	885.25	24.98	4.99	1.817	250	0	875.00	24.99	4.98
1/23/2017	M-10	892.93	24.98	5.00	1.825	100	0	887.28	24.99	5.00
1/24/2017	M-11	896.32	24.94	5.00	1.828	200	0	887.89	24.95	5.01
1/30/2017	M-12	892.51	24.99	4.99	1.824	400	0	885.06	25.00	4.99
2/1/2017	M-13	897.79	24.97	5.01	1.823	400	0	881.13	24.99	5.02
2/3/2017	M-14	898.83	24.99	5.02	1.815	600	0	871.03	24.99	5.02
2/6/2017	M-15	896.01	25.01	5.02	1.815	50	0	894.67	24.99	4.99
2/8/2017	M-16	883.06	25.01	4.97	1.819	150	0	873.99	24.99	4.97
2/9/2017	M-17	896.99	24.98	5.01	1.821	0	0	896.13	25.00	5.01
2/13/2017	M-18	881.95	24.99	4.99	1.806	650	0	853.15	25.00	4.98
2/20/2017	M-19	891.34	24.98	5.00	1.816	30	0	889.79	24.98	5.00
2/23/2017	M-20	891.64	24.96	5.01	1.815	80	0	884.68	24.97	4.99
2/24/2017	M-21	897.89	25.01	5.02	1.819	0	0	896.97	25.01	5.02

Test Date	Specimen ID	BEFORE TEST			CONDITIONS			AFTER TEST			
		Weight mg	Average L mm	Average D mm	Density g/cm ³	P _{H₂O} Pa	P _{H₂} Pa	Weight mg	Average L mm	Average D mm	Density g/cm ³
2/27/2017	M-22	895.83	25.04	5.01	1.818	700	0	872.35	25.11	5.02	1.759
2/28/2017	M-23	890.69	25.03	5.00	1.816	35	0	890.09	25.03	5.00	1.816
3/1/2017	M-24	898.05	25.03	5.02	1.812	35	0	896.31	25.04	5.03	1.806
3/8/2017	M-25	903.07	25.00	5.03	1.820	300	15	890.51	25.00	5.04	1.788
3/9/2017	M-26	890.22	24.98	5.00	1.819	100	30	886.96	25.00	4.99	1.813
3/13/2017	M-27	897.72	24.99	5.02	1.818	50	45	892.03	25.00	5.02	1.806
3/14/2017	M-28	892.03	24.98	5.00	1.822	20	90	891.38	24.99	4.99	1.823
3/16/2017	M-29	899.59	25.00	5.01	1.826	3	15	899.40	25.01	5.00	1.832
3/20/2017	M-30	897.05	24.98	5.02	1.818	300	30	888.89	24.98	5.01	1.810
3/21/2017	M-31	903.81	25.00	5.03	1.819	100	45	900.99	25.01	5.02	1.822
3/23/2017	M-32	893.97	24.99	5.00	1.821	50	90	893.67	25.00	5.00	1.821
3/24/2017	M-33	899.54	24.98	5.02	1.820	3	15	899.19	24.99	5.03	1.814
4/25/2017	M-34	892.36	25.00	5.00	1.820	20	15	891.33	25.01	4.99	1.821
5/1/2017	M-35	894.61	25.00	5.01	1.819	20	15	893.95	25.00	5.00	1.820
5/4/2017	M-36	890.26	24.99	5.00	1.819	300	45	889.96	25.00	4.99	1.818
5/8/2017	M-37	901.42	24.99	5.02	1.823	300	45	889.29	25.00	5.01	1.803
5/10/2017	M-38	905.69	24.98	5.01	1.842	100	90	904.82	25.02	5.04	1.814
5/11/2017	M-39	895.31	25.00	5.01	1.820	50	30	894.79	24.98	4.99	1.833
5/15/2017	M-40	896.80	24.99	5.01	1.820	50	15	895.99	25.00	5.02	1.814
5/16/2017	M-41	894.64	24.98	5.01	1.819	20	30	894.04	24.99	5.01	1.815
5/18/2017	M-42	901.59	24.97	5.03	1.817	300	90	898.47	24.99	5.03	1.811
5/22/2017	M-43	893.54	24.97	5.00	1.822	100	15	891.17	24.99	5.00	1.814
6/14/2017	M-44	892.82	24.96	4.99	1.827	300	0	849.08	24.97	4.99	1.743
6/26/2017	M-45	895.20	25.00	5.00	1.825	300	0	849.92	24.97	4.95	1.770
6/30/2017	M-46	895.65	24.98	5.01	1.820	300	0	848.38	24.98	5.01	1.727
8/3/2017	M-47	889.58	24.99	4.99	1.821	300	0	837.49	24.98	4.98	1.724

APPENDIX B
LOG OF EXPERIMENTAL RESULTS

Data No.	Test date	Spec. ID	P_{H_2O}			Temp	Weight		Time in test		Rate	Weight loss		Preparation			Notes
			target		actual		before	after	before	after		before	after	time	temp	wt. loss	
			Pa	Pa	Pa		°C	mg	mg	h		s ⁻¹	%	%	h	°C	mg
1	11/17/16	M-1	200	202	0	800	897.04	897.02	5.91	8.34	3.19E-09	0.000	0.003	1	1200	0.050	
2	11/17/16	M-1	200	181	0	850	897.02	896.97	8.83	11.40	5.66E-09	0.003	0.008	1	1200	0.050	
3	11/17/16	M-1	200	191	0	900	896.97	896.89	11.92	14.42	1.04E-08	0.008	0.017	1	1200	0.050	
4	11/17/16	M-1	200	191	0	950	896.89	896.65	14.91	17.54	2.86E-08	0.017	0.044	1	1200	0.050	
5	11/17/16	M-1	200	193	0	1000	896.65	895.89	18.03	20.67	8.82E-08	0.044	0.128	1	1200	0.050	
6	11/17/16	M-1	200	193	0	1050	895.89	893.60	21.09	23.69	2.73E-07	0.128	0.384	1	1200	0.050	
7	11/17/16	M-1	200	179	1	1100	893.60	888.15	24.14	26.97	5.99E-07	0.384	0.992	1	1200	0.050	
8	11/21/16	M-2	200	225	0	800	900.94	900.92	5.46	7.24	3.64E-09	0.000	0.002	1	1200	0.078	
9	11/21/16	M-2	200	238	0	850	900.92	900.87	7.79	10.41	5.77E-09	0.002	0.008	1	1200	0.078	
10	11/21/16	M-2	200	245	0	900	900.87	900.80	10.91	13.43	8.44E-09	0.008	0.015	1	1200	0.078	
11	11/21/16	M-2	200	244	0	950	900.80	900.65	13.92	16.57	1.70E-08	0.015	0.032	1	1200	0.078	
12	11/21/16	M-2	200	243	0	1000	900.65	900.11	17.06	19.52	6.76E-08	0.032	0.091	1	1200	0.078	
13	11/21/16	M-2	200	216	0	1050	900.11	897.98	20.14	22.76	2.51E-07	0.091	0.328	1	1200	0.078	
14	11/21/16	M-2	200	220	1	1100	897.98	892.42	23.04	25.93	5.95E-07	0.328	0.945	1	1200	0.078	
15	11/23/16	M-3	100	135	0	800	901.65	901.62	4.84	7.24	2.95E-09	0.000	0.003	1	1200	0.089	
16	11/23/16	M-3	100	135	0	850	901.62	901.58	7.68	10.49	5.04E-09	0.003	0.008	1	1200	0.089	
17	11/23/16	M-3	100	138	0	900	901.58	901.52	10.83	13.43	6.99E-09	0.008	0.014	1	1200	0.089	
18	11/23/16	M-3	100	130	0	950	901.52	901.40	13.89	18.55	8.07E-09	0.014	0.028	1	1200	0.089	

Data No.	Test date	Spec. ID	P _{H₂O}		P _{H₂}	Temp	Weight		Time in test		Rate	Weight loss		Preparation		Notes
			target	actual			before	after	before	after		before	after	time	temp	
			Pa	Pa	Pa	°C	mg	mg	h	h	s ⁻¹	%	%	h	°C	mg
19	11/23/16	M-3	100	122	0	1000	901.40	901.02	17.05	19.68	4.48E-08	0.028	0.070	1	1200	0.089
20	11/23/16	M-3	100	120	0	1050	901.02	899.81	20.14	22.64	1.48E-07	0.070	0.203	1	1200	0.089
21	11/23/16	M-3	100	120	1	1100	899.81	896.67	23.11	25.83	3.57E-07	0.203	0.552	1	1200	0.089
22	11/30/16	M-4	50	56	0	800	900.26	900.24	6.07	7.95	3.28E-09	0.000	0.002	1	1200	0.057
23	11/30/16	M-4	50	57	0	850	900.24	900.19	8.27	10.97	5.49E-09	0.002	0.008	1	1200	0.057
24	11/30/16	M-4	50	56	0	900	900.19	900.13	11.26	14.00	6.98E-09	0.008	0.014	1	1200	0.057
25	11/30/16	M-4	50	56	0	950	900.13	900.03	14.44	17.12	1.14E-08	0.014	0.025	1	1200	0.057
26	11/30/16	M-4	50	56	0	1000	900.03	899.83	17.66	20.14	2.46E-08	0.025	0.047	1	1200	0.057
27	11/30/16	M-4	50	56	0	1050	899.83	899.27	20.62	23.17	6.82E-08	0.047	0.110	1	1200	0.057
28	11/30/16	M-4	50	56	0	1100	899.27	897.57	23.55	26.44	1.81E-07	0.110	0.298	1	1200	0.057
29	12/15/16	M-5	150	154	0	800	885.91	885.88	6.11	7.79	5.79E-09	0.000	0.003	1	1200	0.176
30	12/15/16	M-5	150	163	0	850	885.88	885.82	8.30	10.82	6.84E-09	0.003	0.010	1	1200	0.176
31	12/15/16	M-5	150	163	0	900	885.82	885.74	11.39	14.00	1.05E-08	0.010	0.020	1	1200	0.176
32	12/15/16	M-5	150	162	0	950	885.74	885.59	14.38	16.93	1.78E-08	0.020	0.036	1	1200	0.176
33	12/15/16	M-5	150	155	0	1000	885.59	885.12	17.50	20.14	5.66E-08	0.036	0.090	1	1200	0.176
34	12/15/16	M-5	150	159	0	1050	885.12	883.67	20.59	23.01	1.87E-07	0.090	0.253	1	1200	0.176
35	12/15/16	M-5	150	161	0	1100	883.67	879.93	23.61	26.38	4.24E-07	0.253	0.674	1	1200	0.176
36	12/19/16	M-6	25	28	0	800	895.91	895.89	5.19	7.68	3.24E-09	0.000	0.003	1	1200	0.080
37	12/19/16	M-6	25	18	0	850	895.89	895.84	8.35	10.80	5.95E-09	0.003	0.008	1	1200	0.080
38	12/19/16	M-6	25	18	0	900	895.84	895.78	11.58	13.89	8.46E-09	0.008	0.015	1	1200	0.080
39	12/19/16	M-6	25	18	0	950	895.78	895.69	14.41	16.90	1.10E-08	0.015	0.025	1	1200	0.080
40	12/19/16	M-6	25	18	0	1000	895.69	895.55	17.53	20.09	1.64E-08	0.025	0.040	1	1200	0.080
41	12/19/16	M-6	25	18	0	1050	895.55	895.28	20.65	23.32	3.18E-08	0.040	0.071	1	1200	0.080
42	12/19/16	M-6	25	18	0	1100	895.28	894.68	23.51	26.22	6.85E-08	0.071	0.137	1	1200	0.080
43	12/21/16	M-7	500	416	0	800	886.79	886.78	5.66	7.10	2.18E-09	0.007	0.009	1	1200	0.112
44	12/21/16	M-7	500	420	0	850	886.78	886.75	8.63	10.52	5.80E-09	0.009	0.013	1	1200	0.112

Data No.	Test date	Spec. ID	P _{H₂O}		P _{H₂}	Temp	Weight		Time in test		Rate	Weight loss		Preparation		Notes
			target	actual			before	after	before	after		before	after	time	temp	
			Pa	Pa	Pa	°C	mg	mg	h	h	s ⁻¹	%	%	h	°C	mg
45	12/21/16	M-7	500	453	0	900	886.75	886.72	11.35	12.76	7.55E-09	0.013	0.016	1	1200	0.112
46	12/21/16	M-7	500	455	0	950	886.72	886.67	14.37	15.09	1.78E-08	0.016	0.021	1	1200	0.112
47	12/21/16	M-7	500	629	0	1000	886.67	886.33	19.23	20.01	1.38E-07	0.021	0.060	1	1200	0.112
48	12/21/16	M-7	500	454	0	1050	886.33	885.49	22.32	22.90	4.54E-07	0.060	0.154	1	1200	0.112
49	01/09/17	M-8	25	67	0	800	900.08	900.04	5.21	7.70	4.21E-09	0.039	0.043	1	1200	0.130
50	01/09/17	M-8	25	69	0	850	900.04	899.99	8.32	10.74	6.50E-09	0.043	0.049	1	1200	0.130
51	01/09/17	M-8	25	67	0	900	899.99	899.91	11.36	13.80	9.87E-09	0.049	0.057	1	1200	0.130
52	01/09/17	M-8	25	43	0	950	899.91	899.79	14.42	17.06	1.43E-08	0.057	0.071	1	1200	0.130
53	01/09/17	M-8	25	15	0	1000	899.79	899.65	17.47	19.98	1.76E-08	0.071	0.087	1	1200	0.130
54	01/09/17	M-8	25	15	0	1050	899.65	899.49	21.66	23.14	3.23E-08	0.087	0.104	1	1200	0.130
55	01/09/17	M-8	25	14	0	1100	899.49	899.09	24.24	26.20	6.37E-08	0.104	0.149	1	1200	0.130
56	01/12/17	M-9	250	262	0	800	884.96	884.94	4.64	7.67	1.45E-09	0.033	0.035	1	1200	0.084
57	01/12/17	M-9	250	276	0	850	884.94	884.92	8.24	10.66	3.76E-09	0.035	0.038	1	1200	0.084
58	01/12/17	M-9	250	292	0	900	884.92	884.86	11.50	13.92	6.75E-09	0.038	0.044	1	1200	0.084
59	01/12/17	M-9	250	298	0	950	884.86	884.72	14.41	17.01	1.68E-08	0.044	0.059	1	1200	0.084
60	01/12/17	M-9	250	276	0	1000	884.72	884.15	17.84	20.05	8.23E-08	0.059	0.125	1	1200	0.084
61	01/12/17	M-9	250	264	0	1050	884.15	882.12	20.79	23.00	2.88E-07	0.125	0.354	1	1200	0.084
62	01/12/17	M-9	250	266	0	1100	882.12	876.97	23.66	26.21	6.35E-07	0.354	0.935	1	1200	0.084
63	01/23/17	M-10	100	112	0	800	892.79	892.76	4.70	7.57	3.36E-09	0.000	0.003	1	1200	0.102
64	01/23/17	M-10	100	117	0	850	892.76	892.72	8.23	10.78	5.25E-09	0.003	0.008	1	1200	0.102
65	01/23/17	M-10	100	117	0	900	892.72	892.64	11.38	13.73	9.40E-09	0.008	0.016	1	1200	0.102
66	01/23/17	M-10	100	114	0	950	892.64	892.52	14.53	16.98	1.52E-08	0.016	0.030	1	1200	0.102
67	01/23/17	M-10	100	110	0	1000	892.52	892.22	17.90	20.00	4.45E-08	0.030	0.063	1	1200	0.102
68	01/23/17	M-10	100	108	0	1050	892.22	891.10	20.55	23.08	1.39E-07	0.063	0.190	1	1200	0.102
69	01/23/17	M-10	100	108	0	1100	891.10	888.71	23.88	26.17	3.25E-07	0.190	0.457	1	1200	0.102
70	01/25/17	M-11	200	204	0	800	896.29	896.25	4.78	7.73	3.47E-09	0.000	0.004	1	1200	0.094

Data No.	Test date	Spec. ID	P _{H₂O}		P _{H₂}	Temp	Weight		Time in test		Rate	Weight loss		Preparation		Notes
			target	actual			before	after	before	after		before	after	time	temp	
			Pa	Pa	Pa	°C	mg	mg	h	h	s ⁻¹	%	%	h	°C	mg
71	01/25/17	M-11	200	210	0	850	896.25	896.21	8.27	10.82	5.47E-09	0.004	0.009	1	1200	0.094
72	01/25/17	M-11	200	210	0	900	896.21	896.14	11.38	13.83	8.60E-09	0.009	0.016	1	1200	0.094
73	01/25/17	M-11	200	208	0	950	896.14	896.02	14.65	16.90	1.64E-08	0.016	0.030	1	1200	0.094
74	01/25/17	M-11	200	202	0	1000	896.02	895.63	18.00	19.88	6.55E-08	0.030	0.074	1	1200	0.094
75	01/25/17	M-11	200	196	0	1050	895.63	894.41	21.08	22.72	2.31E-07	0.074	0.210	1	1200	0.094
76	01/25/17	M-11	200	195	0	1100	894.41	890.48	23.88	26.27	5.10E-07	0.210	0.648	1	1200	0.094
77	01/30/17	M-12	400	171	0	800	892.43	892.41	6.03	7.55	3.69E-09	0.009	0.011	1	1200	0.070
78	01/30/17	M-12	400	175	0	850	892.41	892.38	8.48	10.48	5.45E-09	0.011	0.015	1	1200	0.070
79	01/30/17	M-12	400	171	0	900	892.38	892.32	11.47	13.62	8.11E-09	0.015	0.021	1	1200	0.070
80	01/30/17	M-12	400	168	0	950	892.32	892.23	15.15	16.92	1.60E-08	0.021	0.031	1	1200	0.070
81	01/30/17	M-12	400	166	0	1000	892.23	891.88	18.00	19.82	6.02E-08	0.031	0.071	1	1200	0.070
82	01/30/17	M-12	400	167	0	1050	891.88	890.94	21.35	22.77	2.06E-07	0.071	0.176	1	1200	0.070
83	01/30/17	M-12	400	162	0	1100	890.94	889.95	24.38	25.08	4.42E-07	0.176	0.287	1	1200	0.070
84	02/01/17	M-13	400	383	0	800	897.55	897.52	5.53	7.82	3.78E-09	0.000	0.003	1	1200	0.324
85	02/01/17	M-13	400	416	0	850	897.52	897.48	8.28	10.85	5.30E-09	0.003	0.008	1	1200	0.324
86	02/01/17	M-13	400	454	0	900	897.48	897.44	11.55	13.07	7.94E-09	0.008	0.012	1	1200	0.324
87	02/01/17	M-13	400	442	0	950	897.44	897.28	14.55	16.65	2.27E-08	0.012	0.030	1	1200	0.324
88	02/01/17	M-13	400	398	0	1000	897.28	896.91	19.23	20.18	1.21E-07	0.030	0.071	1	1200	0.324
89	02/01/17	M-13	400	381	0	1050	896.91	895.63	22.85	23.33	8.29E-07	0.071	0.214	1	1200	0.324
90	02/01/17	M-13	400	394	0	1100	895.63	890.99	23.58	25.27	8.51E-07	0.214	0.731	1	1200	0.324
91	02/03/17	M-14	600	585	0	800	898.75	898.74	5.18	5.82	5.31E-09	0.009	0.010	1	1200	0.130
92	02/03/17	M-14	600	1060	0	850	898.74	898.71	8.82	10.00	6.81E-09	0.010	0.013	1	1200	0.130
93	02/03/17	M-14	600	1002	0	900	898.71	898.66	11.62	13.95	6.90E-09	0.013	0.019	1	1200	0.130
94	02/03/17	M-14	600	836	0	950	898.66	898.61	16.48	17.00	2.85E-08	0.019	0.024	1	1200	0.130
95	02/03/17	M-14	600	840	0	1000	898.61	898.19	18.93	19.68	1.73E-07	0.024	0.071	1	1200	0.130
96	02/03/17	M-14	600	837	0	1050	898.19	897.30	21.47	21.90	6.44E-07	0.071	0.171	1	1200	0.130

Data No.	Test date	Spec. ID	P _{H₂O}		P _{H₂}	Temp	Weight		Time in test		Rate	Weight loss		Preparation		Notes
			target	actual			before	after	before	after		before	after	time	temp	
			Pa	Pa	Pa	°C	mg	mg	h	h	s ⁻¹	%	%	h	°C	mg
97	02/03/17	M-14	600	829	0	1100	897.30	895.39	24.67	25.02	1.69E-06	0.171	0.383	1	1200	0.130
98	02/06/17	M-15	50	53	0	800	895.68	895.66	5.90	7.73	3.56E-09	0.037	0.039	1	1200	0.120
99	02/06/17	M-15	50	58	0	850	895.66	895.65	10.22	10.93	4.37E-09	0.039	0.041	1	1200	0.120
100	02/06/17	M-15	50	58	0	900	895.65	895.61	11.48	13.20	7.03E-09	0.041	0.045	1	1200	0.120
101	02/06/17	M-15	50	15	0	950	895.61	895.56	15.18	16.78	8.53E-09	0.045	0.050	1	1200	0.120
102	02/06/17	M-15	50	15	0	1000	895.56	895.51	17.52	18.62	1.44E-08	0.050	0.055	1	1200	0.120
103	02/06/17	M-15	50	14	0	1050	895.51	895.45	20.62	21.42	2.52E-08	0.055	0.063	1	1200	0.120
104	02/06/17	M-15	50	14	0	1100	895.45	895.22	24.95	26.27	5.36E-08	0.063	0.088	1	1200	0.120
105	02/08/17	M-16	150	149	0	800	833.43	833.41	5.67	7.64	3.38E-09	-0.045	-0.042	1	1200	-0.647
106	02/08/17	M-16	150	157	0	850	833.41	833.38	8.73	10.37	6.71E-09	-0.042	-0.039	1	1200	-0.647
107	02/08/17	M-16	150	165	0	900	833.38	833.35	11.91	12.98	1.06E-08	-0.039	-0.034	1	1200	-0.647
108	02/08/17	M-16	150	167	0	950	833.35	833.23	14.67	16.52	2.16E-08	-0.034	-0.020	1	1200	-0.647
109	02/08/17	M-16	150	165	0	1000	833.23	832.73	18.19	19.94	9.54E-08	-0.020	0.040	1	1200	-0.647
110	02/08/17	M-16	150	164	0	1050	832.73	832.03	22.27	23.08	2.85E-07	0.040	0.123	1	1200	-0.647
111	02/08/17	M-16	150	162	0	1100	832.03	830.05	24.54	25.73	5.57E-07	0.123	0.361	1	1200	-0.647
112	02/09/17	M-17	0	0	0	800	896.80	896.78	5.37	7.50	2.47E-09	0.021	0.023	1	1200	0.079
113	02/09/17	M-17	0	0	0	850	896.78	896.76	8.53	10.50	4.56E-09	0.023	0.026	1	1200	0.079
114	02/09/17	M-17	0	0	0	900	896.76	896.73	12.17	13.68	5.74E-09	0.026	0.029	1	1200	0.079
115	02/09/17	M-17	0	0	0	950	896.73	896.69	15.05	16.87	5.96E-09	0.029	0.033	1	1200	0.079
116	02/09/17	M-17	0	0	0	1000	896.69	896.66	18.62	19.83	8.19E-09	0.033	0.037	1	1200	0.079
117	02/09/17	M-17	0	0	0	1050	896.66	896.61	21.60	23.08	1.11E-08	0.037	0.043	1	1200	0.079
118	02/09/17	M-17	0	0	0	1100	896.61	896.54	24.78	26.08	1.72E-08	0.043	0.051	1	1200	0.079
119	02/16/17	M-18	650	703	0	800	881.87	881.86	5.28	6.02	3.41E-09	0.009	0.010	1	1200	0.078
120	02/16/17	M-18	650	1125	0	850	881.86	881.84	8.20	9.72	4.97E-09	0.010	0.013	1	1200	0.078
121	02/16/17	M-18	650	1149	0	900	881.84	881.81	12.70	14.07	7.59E-09	0.013	0.016	1	1200	0.078
122	02/16/17	M-18	650	1053	0	950	881.81	881.78	15.77	16.05	2.48E-08	0.016	0.019	1	1200	0.078

Data No.	Test date	Spec. ID	P _{H₂O}		P _{H₂}	Temp	Weight		Time in test		Rate	Weight loss		Preparation		Notes
			target	actual			before	after	before	after		before	after	time	temp	
			Pa	Pa	Pa	°C	mg	mg	h	h	s ⁻¹	%	%	h	°C	mg
123	02/16/17	M-18	650	1231	0	1000	881.78	881.61	19.32	19.60	1.98E-07	0.019	0.039	1	1200	0.078
124	02/16/17	M-18	650	1111	0	1050	881.61	880.71	21.32	21.73	6.88E-07	0.039	0.140	1	1200	0.078
125	02/16/17	M-18	650	973	0	1100	880.71	879.79	24.10	24.27	1.71E-06	0.140	0.245	1	1200	0.078
126	02/20/17	M-19	30	22	0	800	891.36	891.33	4.83	7.65	3.65E-09	-0.002	0.002	1	1200	0.073
127	02/20/17	M-19	30	19	0	850	891.33	891.28	8.57	10.82	6.09E-09	0.002	0.007	1	1200	0.073
128	02/20/17	M-19	30	9	0	900	891.28	891.23	11.43	13.73	7.05E-09	0.007	0.012	1	1200	0.073
129	02/20/17	M-19	30	8	0	950	891.23	891.16	14.65	16.90	9.28E-09	0.012	0.020	1	1200	0.073
130	02/20/17	M-19	30	8	0	1000	891.16	891.06	17.72	20.07	1.37E-08	0.020	0.031	1	1200	0.073
131	02/20/17	M-19	30	9	0	1050	891.06	890.89	20.72	22.95	2.32E-08	0.031	0.050	1	1200	0.073
132	02/20/17	M-19	30	9	0	1100	890.89	890.67	24.15	25.82	4.16E-08	0.050	0.075	1	1200	0.073
133	02/23/17	M-20	80	76	0	800	891.48	891.42	5.08	7.63	7.45E-09	0.018	0.025	1	1200	0.181
134	02/23/17	M-20	80	76	0	850	891.42	891.35	8.43	10.82	9.13E-09	0.025	0.033	1	1200	0.181
135	02/23/17	M-20	80	77	0	900	891.35	891.24	11.52	13.75	1.52E-08	0.033	0.045	1	1200	0.181
136	02/23/17	M-20	80	76	0	950	891.24	890.99	14.67	16.77	3.71E-08	0.045	0.073	1	1200	0.181
137	02/23/17	M-20	80	76	0	1000	890.99	890.33	17.75	20.12	8.67E-08	0.073	0.147	1	1200	0.181
138	02/23/17	M-20	80	75	0	1050	890.33	889.14	20.87	23.10	1.67E-07	0.147	0.281	1	1200	0.181
139	02/23/17	M-20	80	76	0	1100	889.14	886.79	23.97	26.17	3.34E-07	0.281	0.544	1	1200	0.181
140	02/24/17	M-21	0	0	0	800	897.87	897.84	4.62	7.32	3.21E-09	0.002	0.006	1	1200	0.087
141	02/24/17	M-21	0	0	0	850	897.84	897.80	8.33	10.62	5.40E-09	0.006	0.010	1	1200	0.087
142	02/24/17	M-21	0	0	0	900	897.80	897.77	11.65	12.97	6.09E-09	0.010	0.013	1	1200	0.087
143	02/24/17	M-21	0	0	0	950	897.77	897.75	16.13	17.12	6.25E-09	0.013	0.015	1	1200	0.087
144	02/24/17	M-21	0	0	0	1000	897.75	897.70	17.88	19.88	7.74E-09	0.015	0.021	1	1200	0.087
145	02/24/17	M-21	0	0	0	1050	897.70	897.63	20.87	22.98	1.09E-08	0.021	0.029	1	1200	0.087
146	02/24/17	M-21	0	0	0	1100	897.63	897.51	23.90	26.10	1.65E-08	0.029	0.042	1	1200	0.087
147	02/27/17	M-22	700	670	0	800	895.84	895.83	6.32	7.15	5.60E-09	-0.001	0.000	1	1200	0.015
148	02/27/17	M-22	700	968	0	850	895.83	895.82	8.27	8.67	1.55E-09	0.000	0.001	1	1200	0.015

Data No.	Test date	Spec. ID	P _{H₂O}		P _{H₂}	Temp	Weight		Time in test		Rate	Weight loss		Preparation		Notes
			target	actual			before	after	before	after		before	after	time	temp	
			Pa	Pa	Pa	°C	mg	mg	h	h	s ⁻¹	%	%	h	°C	mg
149	02/27/17	M-22	700	1033	0	900	895.82	895.81	11.87	12.67	5.81E-09	0.001	0.002	1	1200	0.015
150	02/27/17	M-22	700	986	0	950	895.81	895.76	14.35	15.10	1.94E-08	0.002	0.008	1	1200	0.015
151	02/27/17	M-22	700	977	0	1000	895.76	894.92	17.52	19.28	1.48E-07	0.008	0.101	1	1200	0.015
152	02/27/17	M-22	700	983	0	1050	894.92	892.91	21.07	22.02	6.57E-07	0.101	0.326	1	1200	0.015
153	02/27/17	M-22	700	899	0	1100	892.91	886.03	23.78	25.08	1.65E-06	0.326	1.094	1	1200	0.015
154	02/28/17	M-23	35	3	0	800	890.59	890.56	5.00	7.40	4.03E-09	0.012	0.015	1	1200	0.115
155	02/28/17	M-23	35	4	0	850	890.56	890.52	8.52	10.62	4.60E-09	0.015	0.019	1	1200	0.115
156	02/28/17	M-23	35	4	0	900	890.52	890.49	11.68	13.68	4.83E-09	0.019	0.022	1	1200	0.115
157	03/01/17	M-24	35	30	0	800	897.99	897.98	6.17	7.82	2.44E-09	0.007	0.008	1	1200	0.050
158	03/01/17	M-24	35	31	0	850	897.98	897.96	8.55	9.60	4.12E-09	0.008	0.010	1	1200	0.050
159	03/01/17	M-24	35	31	0	900	897.96	897.95	12.00	12.82	4.15E-09	0.010	0.011	1	1200	0.050
160	03/01/17	M-24	35	30	0	950	897.95	897.92	14.88	16.48	5.99E-09	0.011	0.014	1	1200	0.050
161	03/01/17	M-24	35	30	0	1000	897.92	897.85	18.03	19.67	1.34E-08	0.014	0.022	1	1200	0.050
162	03/01/17	M-24	35	31	0	1050	897.85	897.74	22.15	23.10	3.75E-08	0.022	0.035	1	1200	0.050
163	03/01/17	M-24	35	29	0	1100	897.74	897.37	24.53	25.75	9.33E-08	0.035	0.076	1	1200	0.050
164	03/08/17	M-25	300	302	12	800	903.05	903.05	5.88	6.58	2.20E-09	0.003	0.003	1	1200	0.028
165	03/08/17	M-25	300	305	12	850	903.05	903.04	8.37	9.23	1.79E-09	0.003	0.004	1	1200	0.028
166	03/08/17	M-25	300	330	12	900	903.04	903.02	11.77	13.80	3.18E-09	0.004	0.006	1	1200	0.028
167	03/08/17	M-25	300	349	12	950	903.02	902.92	14.78	16.88	1.54E-08	0.006	0.018	1	1200	0.028
168	03/08/17	M-25	300	368	12	1000	902.92	902.69	17.70	18.67	7.23E-08	0.018	0.043	1	1200	0.028
169	03/08/17	M-25	300	388	12	1050	902.69	902.21	21.38	21.80	3.51E-07	0.043	0.096	1	1200	0.028
170	03/08/17	M-25	300	329	12	1100	902.21	898.69	24.12	25.50	7.85E-07	0.096	0.486	1	1200	0.028
171	03/09/17	M-26	100	125	25	800	890.16	890.16	6.32	7.17	1.10E-09	-0.361	-0.361	1	1200	0.028
172	03/09/17	M-26	100	267	25	850	890.16	890.16	10.17	10.78	2.56E-09	-0.361	-0.360	1	1200	0.028
173	03/09/17	M-26	100	131	25	900	890.16	890.15	13.22	13.92	8.92E-10	-0.360	-0.360	1	1200	0.028
174	03/09/17	M-26	100	127	25	950	890.15	890.13	14.75	16.62	3.17E-09	-0.360	-0.358	1	1200	0.028

Data No.	Test date	Spec. ID	P _{H₂O}		P _{H₂}	Temp	Weight		Time in test		Rate	Weight loss		Preparation		Notes	
			target	actual			before	after	before	after		before	after	time	temp		
			Pa	Pa	Pa	°C	mg	mg	h	h	s ⁻¹	%	%	h	°C	mg	
175	03/09/17	M-26	100	119	25	1000	890.13	890.05	17.77	19.37	1.70E-08	-0.358	-0.348	1	1200	0.028	
176	03/09/17	M-26	100	117	25	1050	890.05	889.75	21.58	22.88	7.23E-08	-0.348	-0.314	1	1200	0.028	
177	03/09/17	M-26	100	119	25	1100	889.75	888.19	24.40	26.05	2.95E-07	-0.314	-0.139	1	1200	0.028	
178	03/13/17	M-27	50	49	38	800	890.16	890.16	5.20	7.30	1.93E-09	0.209	0.210	1	1200	0.028	
179	03/13/17	M-27	50	44	36	850	890.16	890.16	8.63	10.18	1.61E-09	0.210	0.210	1	1200	0.028	
180	03/13/17	M-27	50	24	38	900	890.16	890.15	12.42	13.57	-2.71E-10	0.210	0.210	1	1200	0.028	R
181	03/13/17	M-27	50	22	36	950	890.15	890.13	15.03	16.90	5.01E-10	0.210	0.213	1	1200	0.028	
182	03/13/17	M-27	50	22	37	1000	890.13	890.05	17.87	19.82	2.24E-09	0.213	0.222	1	1200	0.028	
183	03/13/17	M-27	50	22	37	1050	890.05	889.75	20.97	22.85	6.14E-09	0.222	0.256	1	1200	0.028	
184	03/13/17	M-27	50	22	38	1100	889.75	888.19	23.85	26.23	1.47E-08	0.256	0.431	1	1200	0.028	
185	03/14/17	M-28	20	23	100	800	892.09	892.09	5.90	7.68	2.20E-09	-0.080	-0.079	1	1200	0.028	UR
186	03/14/17	M-28	20	23	100	850	892.09	892.09	8.52	10.80	1.79E-09	-0.079	-0.079	1	1200	0.028	UR
187	03/14/17	M-28	20	23	100	900	892.09	892.08	11.47	13.73	3.18E-09	-0.079	-0.079	1	1200	0.028	UR
188	03/14/17	M-28	20	23	100	950	892.08	892.08	14.80	17.00	1.54E-08	-0.079	-0.079	1	1200	0.028	UR
189	03/14/17	M-28	20	23	100	1000	892.08	892.06	17.72	19.90	7.23E-08	-0.079	-0.077	1	1200	0.028	UR
190	03/14/17	M-28	20	23	100	1050	892.06	891.99	20.68	23.08	3.51E-07	-0.077	-0.068	1	1200	0.028	UR
191	03/14/17	M-28	20	23	100	1100	891.99	891.83	23.67	25.97	7.85E-07	-0.068	-0.051	1	1200	0.028	UR
192	03/16/17	M-29	3	3	46	800	899.57	899.54	4.84	7.24	2.20E-09	-1.122	-1.119	1	1200	0.028	UR
193	03/16/17	M-29	3	3	46	850	899.54	899.50	7.68	10.49	1.79E-09	-1.119	-1.114	1	1200	0.028	UR
194	03/16/17	M-29	3	3	46	900	899.50	899.44	10.83	13.43	3.18E-09	-1.114	-1.107	1	1200	0.028	UR
195	03/16/17	M-29	3	3	46	950	899.44	899.32	13.89	16.55	1.54E-08	-1.107	-1.093	1	1200	0.028	UR
196	03/16/17	M-29	3	3	46	1000	899.32	898.94	17.05	19.68	7.23E-08	-1.093	-1.050	1	1200	0.028	UR
197	03/16/17	M-29	3	3	46	1050	898.94	897.73	20.14	22.64	3.51E-07	-1.050	-0.915	1	1200	0.028	UR
198	03/16/17	M-29	3	3	46	1100	897.73	894.59	23.11	25.83	7.85E-07	-0.915	-0.562	1	1200	0.028	UR
199	03/20/17	M-30	300	294	25	800	896.72	896.71	6.10	7.52	1.53E-09	0.037	0.038	1	1200	0.059	
200	03/20/17	M-30	300	296	25	850	896.71	896.71	8.27	10.43	8.60E-10	0.038	0.038	1	1200	0.059	

Data No.	Test date	Spec. ID	P _{H₂O}		P _{H₂}	Temp	Weight		Time in test		Rate	Weight loss		Preparation		Notes
			target	actual			before	after	before	after		before	after	time	temp	
			Pa	Pa	Pa	°C	mg	mg	h	h	s ⁻¹	%	%	h	°C	mg
201	03/20/17	M-30	300	315	25	900	896.71	896.70	11.43	13.27	1.52E-09	0.038	0.039	1	1200	0.059
202	03/20/17	M-30	300	327	25	950	896.70	896.67	14.93	16.60	5.75E-09	0.039	0.043	1	1200	0.059
203	03/20/17	M-30	300	341	25	1000	896.67	896.45	17.77	19.73	3.40E-08	0.043	0.067	1	1200	0.059
204	03/20/17	M-30	300	325	25	1050	896.45	895.49	21.62	23.10	2.01E-07	0.067	0.173	1	1200	0.059
205	03/20/17	M-30	300	311	25	1100	895.49	894.08	25.37	26.15	5.64E-07	0.173	0.332	1	1200	0.059
206	03/21/17	M-31	100	169	39	800	903.72	903.71	5.52	7.62	4.39E-10	0.010	0.011	1	1200	0.082
207	03/21/17	M-31	100	171	39	850	903.71	903.71	9.52	10.73	2.54E-10	0.011	0.011	1	1200	0.082
208	03/21/17	M-31	100	172	39	900	903.71	903.71	11.62	13.47	1.66E-10	0.011	0.011	1	1200	0.082
209	03/21/17	M-31	100	167	39	950	903.71	903.70	14.98	16.87	1.79E-09	0.011	0.012	1	1200	0.082
210	03/21/17	M-31	100	152	39	1000	903.70	903.65	17.95	19.83	8.99E-09	0.012	0.018	1	1200	0.082
211	03/21/17	M-31	100	165	39	1050	903.65	903.40	21.80	23.15	5.62E-08	0.018	0.045	1	1200	0.082
212	03/21/17	M-31	100	153	39	1100	903.40	902.60	24.73	26.03	1.88E-07	0.045	0.134	1	1200	0.082
213	03/23/17	M-32	50	62	100	800	893.92	893.91	5.10	7.48	1.04E-09	0.005	0.006	1	1200	0.050
214	03/23/17	M-32	50	68	100	850	893.91	893.92	8.57	10.68	-4.42E-10	0.006	0.006	1	1200	0.050 R
215	03/23/17	M-32	50	59	100	900	893.92	893.92	11.98	13.87	-1.64E-10	0.006	0.006	1	1200	0.050 R
216	03/23/17	M-32	50	33	100	950	893.92	893.92	14.65	16.85	2.82E-10	0.006	0.006	1	1200	0.050
217	03/23/17	M-32	50	31	100	1000	893.92	893.91	17.93	20.07	1.31E-09	0.006	0.007	1	1200	0.050
218	03/23/17	M-32	50	31	100	1050	893.91	893.87	20.83	22.97	5.52E-09	0.007	0.011	1	1200	0.050
219	03/23/17	M-32	50	31	100	1100	893.87	893.80	23.92	25.55	1.30E-08	0.011	0.019	1	1200	0.050
220	03/24/17	M-33	3	3	11	800	899.50	899.50	5.75	7.62	8.26E-10	0.004	0.005	1	1200	0.042
221	03/24/17	M-33	3	3	11	850	899.50	899.49	8.53	10.72	1.27E-09	0.005	0.006	1	1200	0.042
222	03/24/17	M-33	3	4	11	900	899.49	899.49	11.78	13.68	-1.63E-10	0.006	0.006	1	1200	0.042 R
223	03/24/17	M-33	3	4	11	950	899.49	899.49	15.50	16.95	6.39E-10	0.006	0.006	1	1200	0.042
224	03/24/17	M-33	3	4	11	1000	899.49	899.48	17.93	19.95	6.12E-10	0.006	0.007	1	1200	0.042
225	03/24/17	M-33	3	4	11	1050	899.48	899.47	20.93	23.03	1.18E-09	0.007	0.007	1	1200	0.042
226	03/24/17	M-33	3	3	10	1100	899.47	899.47	23.75	26.12	1.04E-09	0.007	0.008	1	1200	0.042

Data No.	Test date	Spec. ID	P _{H₂O}		P _{H₂}	Temp	Weight		Time in test		Rate	Weight loss		Preparation		Notes	
			target	actual			before	after	before	after		before	after	time	temp		
			Pa	Pa	Pa	°C	mg	mg	h	h	s ⁻¹	%	%	h	°C	mg	
227	04/27/17	M-34	20	3	13	800	892.09	892.08	6.05	7.65	9.73E-10	0.000	0.001	1	1200	0.275	
228	04/27/17	M-34	20	3	13	850	892.08	892.08	8.50	10.82	1.34E-10	0.001	0.001	1	1200	0.275	
229	04/27/17	M-34	20	4	13	900	892.08	892.08	11.88	13.82	-1.61E-10	0.001	0.001	1	1200	0.275	R
230	04/27/17	M-34	20	4	13	950	892.08	892.08	15.08	17.05	9.48E-10	0.001	0.001	1	1200	0.275	
231	04/27/17	M-34	20	4	13	1000	892.08	892.07	18.82	20.08	2.22E-09	0.001	0.002	1	1200	0.275	
232	04/27/17	M-34	20	4	13	1050	892.07	892.04	21.38	22.93	4.82E-09	0.002	0.005	1	1200	0.275	
233	04/27/17	M-34	20	4	13	1100	892.04	891.99	24.02	25.97	9.26E-09	0.005	0.011	1	1200	0.275	
234	05/03/17	M-35	20	4	14	800	894.36	894.35	6.70	7.95	1.49E-09	0.000	0.001	1	1200	0.282	
235	05/03/17	M-35	20	4	14	850	894.35	894.35	9.88	10.83	1.63E-09	0.001	0.001	1	1200	0.282	
236	05/03/17	M-35	20	4	14	900	894.35	894.35	12.08	13.85	0.00E+00	0.001	0.001	1	1200	0.282	R
237	05/03/17	M-35	20	4	14	950	894.35	894.34	15.27	17.13	5.01E-10	0.001	0.002	1	1200	0.282	
238	05/03/17	M-35	20	4	14	1000	894.34	894.34	17.73	19.23	1.24E-09	0.002	0.002	1	1200	0.282	
239	05/03/17	M-35	20	3	14	1050	894.34	894.32	20.80	22.70	2.94E-09	0.002	0.004	1	1200	0.282	
240	05/03/17	M-35	20	3	14	1100	894.32	894.29	24.02	25.93	4.39E-09	0.004	0.007	1	1200	0.282	
241	05/04/17	M-36	300	4	43	800	889.98	889.97	5.12	7.03	2.29E-09	0.000	0.002	1	1200	0.284	
242	05/04/17	M-36	300	4	43	850	889.97	889.96	9.12	10.33	1.29E-09	0.002	0.002	1	1200	0.284	
243	05/04/17	M-36	300	4	42	900	889.96	889.96	11.72	14.02	4.07E-10	0.002	0.002	1	1200	0.284	
244	05/04/17	M-36	300	4	42	950	889.96	889.96	15.78	16.53	4.16E-10	0.002	0.003	1	1200	0.284	
245	05/04/17	M-36	300	4	42	1000	889.96	889.95	17.87	19.17	1.20E-09	0.003	0.003	1	1200	0.284	
246	05/08/17	M-37	300	305	36	800	901.28	901.26	5.08	7.27	2.39E-09	0.000	0.002	1	1200	0.131	
247	05/08/17	M-37	300	341	37	850	901.26	901.25	8.32	10.52	2.38E-09	0.002	0.004	1	1200	0.131	
248	05/08/17	M-37	300	333	34	900	901.25	901.23	11.73	13.60	2.64E-09	0.004	0.006	1	1200	0.131	
249	05/08/17	M-37	300	356	34	950	901.23	901.17	14.67	16.87	8.41E-09	0.006	0.012	1	1200	0.131	
250	05/08/17	M-37	300	346	33	1000	901.17	900.87	17.83	19.97	4.31E-08	0.012	0.045	1	1200	0.131	
251	05/08/17	M-37	300	348	35	1050	900.87	899.12	20.80	23.02	2.44E-07	0.045	0.240	1	1200	0.131	
252	05/08/17	M-37	300	359	37	1100	899.12	893.42	23.73	25.73	8.80E-07	0.240	0.872	1	1200	0.131	

Data No.	Test date	Spec. ID	P _{H₂O}		P _{H₂}	Temp	Weight		Time in test		Rate	Weight loss		Preparation		Notes	
			target	actual			before	after	before	after		before	after	time	temp		
			Pa	Pa	Pa	°C	mg	mg	h	h	s ⁻¹	%	%	h	°C	mg	
253	05/10/17	M-38	100	108	76	800	905.69	905.68	5.85	7.68	1.84E-09	0.000	0.001	1	1200	0.034	
254	05/10/17	M-38	100	108	77	850	905.68	905.67	8.60	10.90	1.20E-09	0.001	0.002	1	1200	0.034	
255	05/10/17	M-38	100	112	76	900	905.67	905.67	11.55	13.55	0.00E+00	0.002	0.002	1	1200	0.034	R
256	05/10/17	M-38	100	114	76	950	905.67	905.67	14.62	16.78	5.68E-10	0.002	0.003	1	1200	0.034	R
257	05/10/17	M-38	100	115	76	1000	905.67	905.65	17.80	19.95	3.00E-09	0.003	0.005	1	1200	0.034	
258	05/10/17	M-38	100	111	76	1050	905.65	905.57	20.83	22.98	1.16E-08	0.005	0.014	1	1200	0.034	
259	05/10/17	M-38	100	110	76	1100	905.57	905.26	24.30	26.08	5.26E-08	0.014	0.048	1	1200	0.034	
260	05/11/17	M-39	50	61	25	800	895.08	895.06	5.12	7.53	2.58E-09	0.000	0.002	1	1200	0.019	
261	05/11/17	M-39	50	39	24	850	895.06	895.05	9.70	10.68	2.53E-09	0.002	0.003	1	1200	0.019	
262	05/11/17	M-39	50	37	24	900	895.05	895.05	12.67	13.73	1.17E-09	0.003	0.004	1	1200	0.019	
263	05/11/17	M-39	50	37	24	950	895.05	895.04	14.73	16.43	5.48E-10	0.004	0.004	1	1200	0.019	
264	05/11/17	M-39	50	37	25	1000	895.04	894.40	18.02	19.95	1.03E-07	0.004	0.076	1	1200	0.019	R
265	05/11/17	M-39	50	37	24	1050	894.40	894.35	20.88	22.97	8.32E-09	0.076	0.082	1	1200	0.019	
266	05/11/17	M-39	50	37	24	1100	894.35	894.20	23.97	25.83	2.49E-08	0.082	0.098	1	1200	0.019	
267	05/15/17	M-40	50	53	12	800	896.80	896.78	6.25	7.82	3.35E-09	0.000	0.002	1	1200	0.014	
268	05/15/17	M-40	50	53	12	850	896.78	896.74	8.63	10.55	6.29E-09	0.002	0.006	1	1200	0.014	
269	05/15/17	M-40	50	53	12	900	896.74	896.73	11.70	13.68	1.56E-09	0.006	0.007	1	1200	0.014	
270	05/15/17	M-40	50	53	12	950	896.73	896.73	14.92	16.75	1.18E-09	0.007	0.008	1	1200	0.014	
271	05/15/17	M-40	50	53	12	1000	896.73	896.71	17.78	19.58	2.75E-09	0.008	0.010	1	1200	0.014	
272	05/15/17	M-40	50	53	12	1050	896.71	896.63	20.88	22.83	1.27E-08	0.010	0.019	1	1200	0.014	
273	05/15/17	M-40	50	53	12	1100	896.63	896.30	23.92	26.08	4.76E-08	0.019	0.056	1	1200	0.014	
274	05/16/17	M-41	20	22	25	800	894.65	894.62	5.13	7.68	3.53E-09	0.000	0.003	1	1200	-0.003	
275	05/16/17	M-41	20	22	25	850	894.62	894.61	8.37	10.45	2.39E-09	0.003	0.005	1	1200	-0.003	
276	05/16/17	M-41	20	33	25	900	894.61	894.59	11.68	13.62	1.92E-09	0.005	0.006	1	1200	-0.003	
277	05/16/17	M-41	20	42	25	950	894.59	894.60	14.58	17.00	-2.57E-10	0.006	0.006	1	1200	-0.003	R
278	05/16/17	M-41	20	47	25	1000	894.60	894.58	17.82	19.95	2.04E-09	0.006	0.008	1	1200	-0.003	

Data No.	Test date	Spec. ID	P _{H₂O}		P _{H₂}	Temp	Weight		Time in test		Rate	Weight loss		Preparation		Notes
			target	actual			before	after	before	after		before	after	time	temp	
			Pa	Pa			Pa	°C	mg	mg		h	h	s ⁻¹	h	
279	05/16/17	M-41	20	52	25	1050	894.58	894.53	20.77	22.85	8.36E-09	0.008	0.014	1	1200	-0.003
280	05/16/17	M-41	20	56	25	1100	894.53	894.30	23.95	26.02	3.36E-08	0.014	0.039	1	1200	-0.003
281	05/18/17	M-42	300	285	76	800	901.64	901.63	4.82	7.35	2.19E-09	0.000	0.002	1	1200	-0.018
282	05/18/17	M-42	300	293	76	850	901.63	901.62	8.47	10.70	1.24E-09	0.002	0.003	1	1200	-0.018
283	05/18/17	M-42	300	297	71	900	901.62	901.62	11.58	13.77	1.41E-10	0.003	0.003	1	1200	-0.018
284	05/18/17	M-42	300	301	71	950	901.62	901.61	14.70	16.60	3.24E-10	0.003	0.003	1	1200	-0.018
285	05/18/17	M-42	300	327	73	1000	901.61	901.59	17.83	19.95	4.21E-09	0.003	0.007	1	1200	-0.018
286	05/18/17	M-42	300	322	73	1050	901.59	901.28	20.75	23.12	4.03E-08	0.007	0.041	1	1200	-0.018
287	05/18/17	M-42	300	326	74	1100	901.28	899.32	23.73	26.08	2.57E-07	0.041	0.258	1	1200	-0.018

Notes: R = data rejected (negative of zero); UR – unreliable data